Low-Temperature Rate Coefficients for Reactions of Ethynyl Radical (C_2H) with Propane, Isobutane, *n*-Butane, and Neopentane

Ray J. Hoobler, Brian J. Opansky, and Stephen R. Leone*,†

JILA, National Institute of Standards and Technology and University of Colorado, Department of Chemistry and Biochemistry, University of Colorado, Boulder, Colorado 80309-0440

Received: October 22, 1996; In Final Form: December 6, 1996[⊗]

Low-temperature rate coefficients for the reactions of $C_2H + RH \rightarrow$ products (RH = C_3H_8, *i*-C_4H_{10}, *n*-C_4H_{10}, and *neo*-C_5H_{12}) have been measured over the temperature range 154−361 K. Measurements were made using laser photolysis of C_2H_2 to produce C_2H. Transient infrared laser absorption decays of C_2H are used to monitor the subsequent reaction in a transverse flow cell. The results show that the rate coefficients for the reactions of C_2H with propane are independent of temperature while the rate coefficients for the reactions of C_2H with isobutane, *n*-butane, and neopentane have a negative temperature dependence. Over the experimental temperature range, the rate constants for C_2H + RH fit the following Arrhenius expressions: $k_{\text{propane}} = (7.8 \pm 0.4) \times 10^{-11} \exp[(3 \pm 12)/T]$, $k_{\text{isobutane}} = (8.7 \pm 0.8) \times 10^{-11} \exp[(28 \pm 21)/T]$, $k_{n\text{-butane}} = (8.3 \pm 0.6) \times 10^{-11} \exp[(112 \pm 18)/T]$, $k_{\text{neopentane}} = (7.6 \pm 0.9) \times 10^{-11} \exp[(107 \pm 30)/T]$ cm^3 molecules^{-1} s^{-1}. The corresponding rate constants at 298 K are $k_{\text{propane}} = 7.9 \times 10^{-11}$, $k_{\text{isobutane}} = 9.6 \times 10^{-11}$, $k_{n\text{-butane}} = 1.2 \times 10^{-10}$, $k_{\text{neopentane}} = 1.1 \times 10^{-10}$ cm^3 molecules^{-1} s^{-1}.

Introduction

The gas-phase reactions of polyatomic, organic free radicals are of interest in several different research areas including combustion science[1] and terrestrial[2] and planetary atmospheric chemistry.[3] Although the typical kinetics data bases contain a large number of references to studies at and above room temperature, the number of accurate, low-temperature rate coefficients is considerably smaller. Thus, there is a lack of data for detailed complex atmospheric models of the outer planets such as Jupiter, Saturn, and its satellite Titan. Titan is of particular interest because its organic chemistry may be relevant to events leading to the origin of life on Earth.[4] There are two primary post-Voyager models that attempt to discern the photochemistry and development of the atmosphere of Titan.[5,6] Unfortunately, the models rely in many cases on extrapolation from high-temperature results, theory, or estimations of rate coefficients. With the ongoing Galileo mission to Jupiter and the upcoming launch of the Cassini/Huygens mission to Saturn and Titan, the need for more accurate laboratory data will, undoubtedly, become only more apparent.

The current research is focused on the reactivity of the ethynyl radical, C_2H, with three-, four-, and five-carbon atom, saturated hydrocarbons. Ethynyl radical is produced in the planetary atmospheres by photolysis of acetylene. Although propane is the largest unsaturated hydrocarbon detected to date in the atmospheres of Jupiter and Titan,[7] models include C_3 and higher hydrocarbon photochemistry and predict the presence of heavier hydrocarbons as minor constituents. Laboratory simulations of Titan's atmosphere produce a remarkable mixture of C_3−C_6 compounds.[8]

In the photochemical models of Titan, abstraction of hydrogen is a key step in the propagation of free radicals to eventually produce larger organic molecules by radical−radical association reactions. As an illustration, the abstraction of hydrogen from small hydrocarbons methane and ethane by the ethynyl radical results in subsequent recombination of the radical species to form propane:

$$2(C_2H_2 + h\nu \rightarrow C_2H + H) \tag{1}$$

$$C_2H + CH_4 \rightarrow C_2H_2 + CH_3 \tag{2}$$

$$C_2H + C_2H_6 \rightarrow C_2H_2 + C_2H_5 \tag{3}$$

$$CH_3 + C_2H_5 + M \rightarrow C_3H_8 \tag{4}$$

In Toublanc et al.[5] and Yung et al.,[6] propane is destroyed or lost by (i) photolysis,

$$\begin{aligned} C_3H_8 + h\nu &\rightarrow C_3H_6 + H_2 \\ &\rightarrow C_2H_6 + {}^1CH_2 \\ &\rightarrow C_2H_5 + CH_3 \\ &\rightarrow C_2H_4 + CH_4 \end{aligned} \tag{5}$$

(ii) abstraction by C_2H,

$$C_2H + C_3H_8 \rightarrow C_2H_2 + C_3H_7 \tag{6}$$

and (iii) condensation to liquid in the lower stratosphere.

The photochemistries of several C_4 processes, including

$$C_2H + C_4H_{10} \rightarrow C_2H_2 + C_4H_9 \tag{7}$$

are incorporated into the most recent photochemical model of Jupiter.[3] No distinction is made between the two structural isomers for C_4H_{10}.

There is no experimental data on which products are formed, and the C_2H + RH reactions are typically considered to be hydrogen abstraction reactions. Of course, formation of several

---

[†] Staff Member, Quantum Physics Division, National Institute of Standards and Technology.

[⊗] Abstract published in *Advance ACS Abstracts,* January 15, 1997.

S1089-5639(96)03286-0 CCC: $14.00

alkyl radical species is possible for propane, isobutane, and *n*-butane,[9]

$$C_2H + CH_3CH_2CH_3 \rightarrow C_2H_2 + CH_3\dot{C}HCH_3 \qquad \Delta H_{rxn} = -154\ \mathrm{kJ/mol}$$

$$\rightarrow C_2H_2 + CH_3\dot{C}H_2CH \qquad \Delta H_{rxn} = -143\ \mathrm{kJ/mol} \quad (6a)$$

$$C_2H + (CH_3)_3CH \rightarrow C_2H_2 + (CH_3)_3\dot{C} \qquad \Delta H_{rxn} = -165\ \mathrm{kJ/mol}$$

$$\rightarrow C_2H_2 + (CH_3)_2CH\dot{C}H_2 \qquad \Delta H_{rxn} = -145\ \mathrm{kJ/mol} \quad (7a)$$

$$C_2H + CH_3CH_2CH_2CH_3 \rightarrow C_2H_2 + CH_3CH_2\dot{C}HCH_3 \qquad \Delta H_{rxn} = -151\ \mathrm{kJ/mol}$$

$$\rightarrow C_2H_2 + CH_3CH_2CH_2\dot{C}H_2 \qquad \Delta H_{rxn} = -143\ \mathrm{kJ/mol} \quad (7b)$$

while neopentane has only one reaction pathway for hydrogen abstraction.

$$C_2H + (CH_3)_4C \rightarrow C_2H_2 + (CH_3)_3C\dot{C}H_2 \qquad \Delta H_{rxn} = -131\ \mathrm{kJ/mol} \quad (8)$$

Because of the large ΔH_f° of the ethynyl radical (~565 kJ mol^{-1}), an additional addition/elimination pathway is thermodynamically accessible.

$$C_2H + CH_3CH_2CH_3 \rightarrow HC{\equiv}CCH_2CH_2CH_3 + H \qquad \Delta H_{rxn} = -99\ \mathrm{kJ/mol}$$

$$\rightarrow HC{\equiv}CCH(CH_3)_2 + H \qquad \Delta H_{rxn} = -107\ \mathrm{kJ/mol} \quad (9)$$

$$C_2H + (CH_3)_3CH \rightarrow HC{\equiv}CC(CH_3)_3 + H \qquad \Delta H_{rxn} = -115\ \mathrm{kJ/mol}$$

$$\rightarrow HC{\equiv}CCH_2C(CH_3)_2 + H \qquad \Delta H_{rxn} = -96\ \mathrm{kJ/mol} \quad (10)$$

$$C_2H + CH_3CH_2CH_2CH_3 \rightarrow HC{\equiv}CCH(CH_3)CH_2CH_3 + H \qquad \Delta H_{rxn} = -103\ \mathrm{kJ/mol}$$

$$\rightarrow HC{\equiv}CCH_2CH_2CH_2CH_3 + H \qquad \Delta H_{rxn} = -98\ \mathrm{kJ/mol} \quad (11)$$

$$C_2H + C(CH_3)_4 \rightarrow HC{\equiv}CCH_2C(CH_3)_3 + H \qquad \Delta H_{rxn} = -93\ \mathrm{kJ/mol} \quad (12)$$

In this paper, reactions of C_2H with propane, isobutane, *n*-butane, and neopentane are examined and the rate coefficients are determined using transient IR laser absorption spectroscopy. The measured rate coefficients differ by up to an order of magnitude from those previously reported. Although the mixing ratio for higher molecular weight hydrocarbons is relatively small in the planetary atmospheres, the models become increasingly complex with the introduction of C_3 and higher hydrocarbon photochemistry,[3,5,6] including the reactions studied here. The low-temperature rate coefficients will allow for a more refined understanding of the mechanisms of these reactions and their impact on models of the planetary atmospheres.

Experiment

The experimental technique used in the determination of low-temperature rate coefficients of the ethynyl radical has been described in detail,[10,11] and only a brief overview is presented here. The ethynyl radicals are produced by photolysis of acetylene in a flow cell using a pulsed excimer laser operating at 193 nm (70mJ/pulse at 10 Hz). A single-mode F-center laser operating at 3593.68 cm^{-1} probes the transient concentration of C_2H by monitoring the absorption of the $Q_{11}(9)$ line of the $A^2\Pi - X\ ^2\Sigma^+$ (0 0 0) transition. The longitudinal mode structure of the F-center laser is monitored with a scanning Fabry–Perot spectrum analyzer, and a traveling wave meter is used for measuring the wavelength.[12]

The kinetic experiments are performed in a 1 m long, 2.5 cm diameter variable temperature flow cell. The photolysis and probe lasers are overlapped over the full length of the cell, and a three-times multipass of the probe beam is employed to increase the absorption path length. The cell is somewhat unique in that the gases are introduced into and removed from the cell via a series of transverse inlets and pump-outs. This transverse arrangement allows rapid removal of the photolysis products from the probe volume. The cell was cooled by the circulation of pentane or isobutane through an outer jacket after having passed through a copper coil submerged in an ethanol/liquid nitrogen slush bath. Temperatures of ~155 K are easily obtained with this method. Measurements above room temperature to ~360 K are made by circulating water through the outer jacket, while the copper-coils are placed in a water reservoir in which the temperature is controlled by an immersion heater. The temperature in the flow cell is measured by three K-type thermocouples along the length of the cell to ensure that there are no thermal gradients present. Partial pressures of each gas are calculated from the measured flow rates using calibrated mass flow meters and the total pressure. Typical number densities for C_2H_2 and RH are $(2-6) \times 10^{14}$ cm^{-3} and $(0.5-4.5) \times 10^{15}$ cm^{-3}, respectively, with the balance being helium. By use of an absorption cross section at 193 nm of 1.35×10^{-19} cm^{-2} and a quantum yield of 0.26, the upper limit for $[C_2H]$ is estimated to be 6.5×10^{11} cm^{-3}.[13,14] The total pressure for normal data acquisition is between 3.7 and 4.1 kPa (28–31 Torr). Pressure dependence measurements are conducted over the range 1.3–12 kPa (10–90 Torr). All gases are allowed to flow through a mixing cell before entering the low-temperature cell. He (99.99%), C_2H_2 (99.6%), C_3H_8 (99.97%), *n*-C_4H_{10} (99.9%) *i*-C_4H_{10} (99.99%), and *neo*-C_5H_{12} (0.988%) in He are obtained from commercial sources, and all gases are used as received, except acetylene from which acetone was removed by an activated charcoal filter.

The probe beam is directed onto a 50 MHz liquid N_2-cooled Ge:Au detector with a sensitive area of 20 mm^2. The transient signals are amplified and coadded using a digital oscilloscope to improve the signal-to-noise ratio. Samples of 1000–2000 transient absorption signals are averaged before the data are transferred to a personal computer where the data are stored and analyzed.

Results

Rate coefficients are measured under pseudo-first-order conditions where [RH] (RH = C_3H_8, *i*-C_4H_{10}, *n*-C_4H_{10}, and *neo*-C_5H_{12}) and $[C_2H_2] \gg [C_2H]$. The rate of change for $[C_2H]$ can

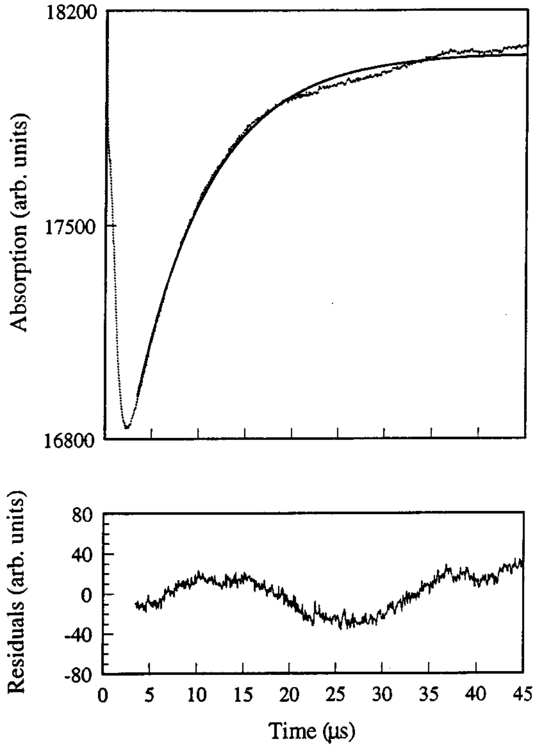

Figure 1. Upper trace: Typical C_2H absorption trace versus time with fit: $T = 210$ K; total pressure = 3.85 kPa; $[C_2H_2] = 4.6 \times 10^{14}$ cm^3 $molecules^{-1}$ s^{-1}; [neopentane] $= 5.1 \times 10^{14}$ cm^3 $molecules^{-1}$ s^{-1}; $k_{obs} = 0.127 \pm 0.001$ μs^{-1} (uncertainty represents 95% confidence limit). Lower trace: Residuals to fitted experimental decay. (Oscillations are due to low-frequency noise from the f-center laser.)

be expressed as

$$d[C_2H]/dt = -[C_2H](k_{RH}[RH] + k_{acetylene}[C_2H_2]) \quad (13)$$

After integration of eq 13,

$$[C_2H] = [C_2H]_0 e^{(-k_{obs})t} \quad (14)$$

where

$$k_{obs} = k_{RH}[RH] + k_{acetylene}[C_2H_2] \quad (15)$$

$$k_{obs} - k_{acetylene}[C_2H_2] = k_{RH}[RH] = k'_{RH} \quad (16)$$

The observed decay rates, k_{obs}, are obtained by fitting the averaged transient signal to the following equation:

$$y = Ae^{-k_{obs}t} + \text{constant} \quad (17)$$

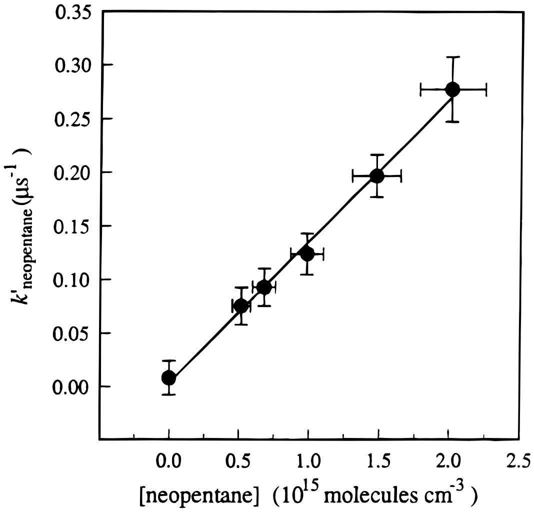

Figure 2. Plot of $k'_{neopentane}$ versus [neopentane]: $T = 210$ K. The rate constant is equal to $(1.33 \pm 0.2) \times 10^{-10}$ cm^3 $molecules^{-1}$ s^{-1}.

TABLE 1: Summary of Rate Constants for C_2H + RH

temp (K)	$k_{propane}$ (cm^3 $molecule^{-1}$ s^{-1})	temp (K)	$k_{n-butane}$ (cm^3 $molecule^{-1}$ s^{-1})
361	$(8.0 \pm 1.3) \times 10^{-11}$	297	$(12.3 \pm 1.6) \times 10^{-11}$
297	$(7.7 \pm 1.2) \times 10^{-11}$	297	$(12.1 \pm 1.5) \times 10^{-11}$
262	$(7.7 \pm 1.0) \times 10^{-11}$	264	$(12.9 \pm 1.4) \times 10^{-11}$
235	$(8.4 \pm 1.2) \times 10^{-11}$	230	$(12.8 \pm 2.1) \times 10^{-11}$
212	$(7.7 \pm 1.0) \times 10^{-11}$	202	$(15.2 \pm 1.8) \times 10^{-11}$
191	$(8.0 \pm 1.5) \times 10^{-11}$	201	$(13.8 \pm 2.0) \times 10^{-11}$
154	$(8.0 \pm 2.2) \times 10^{-11}$	176	$(16.0 \pm 2.0) \times 10^{-11}$

temp (K)	$k_{isobutane}$ (cm^3 $molecule^{-1}$ s^{-1})	temp (K)	$k_{neopentane}$ (cm^3 $molecule^{-1}$ s^{-1})
298	$(9.9 \pm 1.8) \times 10^{-11}$	297	$(10.5 \pm 1.6) \times 10^{-11}$
269	$(9.3 \pm 1.6) \times 10^{-11}$	295	$(10.4 \pm 1.2) \times 10^{-11}$
241	$(9.4 \pm 1.9) \times 10^{-11}$	271	$(12.0 \pm 1.3) \times 10^{-11}$
207	$(10.2 \pm 2.0) \times 10^{-11}$	242	$(12.3 \pm 1.7) \times 10^{-11}$
177	$(10.2 \pm 1.6) \times 10^{-11}$	210	$(13.3 \pm 2.0) \times 10^{-11}$
		181	$(13.1 \pm 1.8) \times 10^{-11}$

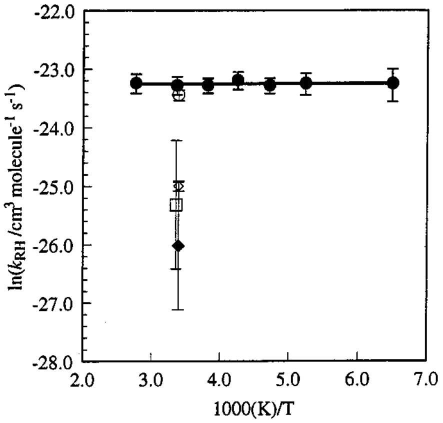

Figure 3. Arrhenius plot, C_2H + propane: ●, this work (Arrhenius fit $k_{propane} = (7.8 \pm 0.4) \times 10^{-11} \exp(3.0 \pm 12/T)$); ◇, Okabe[16] (published value); ○, Okabe[16] (corrected for current $C_2H + C_2H_2$ rate constant of 1.4×10^{-10} cm^3 $molecules^{-1}$ s^{-1}); ◆ Tsang[17] (estimate). For C_2H + isobutane, □ represents Tsang's[18] data (estimate); see Figure 4 for data.

An example of an observed experimental decay and corresponding fit for neopentane is shown in Figure 1. The values of k_{obs} are corrected for the $C_2H + C_2H_2$ contribution by subtraction in eq 16 using the most recent measurements for $k_{acetylene}$.[11,15] The resulting k'_{RH} values are plotted as a function of concentration and fit using a linear least-squares routine. The resultant slope is equal to k_{RH}; this is shown in Figure 2 for neopentane. The uncertainty in k_{RH} is determined by combining the uncertainty in [RH] (which is calculated from the accumulated uncertainties in the instruments used to obtain the pressure, temperature, and flow rate measurements), the uncertainty of the averaged experimental decays, and the uncertainty of the previously measured $k_{acetylene}$.[10,11,15] The relative error in k_{RH} is typically 15−25%. The experimental results are summarized in Table 1. Arrhenius plots for the reactions of C_2H + propane, isobutane and *n*-butane, and neopentane are shown in Figures 3, 4, and 5, respectively. Over the experimental temperature range, the rate constants for C_2H + RH fit the following Arrhenius expressions: $k_{propane} = (7.8 \pm 0.4) \times 10^{-11} \exp[(3 \pm 12)/T]$, $k_{isobutane} = (8.7 \pm 0.8) \times 10^{-11} \exp[(28 \pm 21)/T]$, $k_{n-butane} = (8.3 \pm 0.6) \times 10^{-11} \exp[(112 \pm 18)/T]$, and $k_{neopentane} = (7.6 \pm 0.9) \times 10^{-11} \exp[(107 \pm 30)/T]$ cm^3 $molecules^{-1}$ s^{-1}. The corresponding rate constants at 298 K are $k_{propane} =$

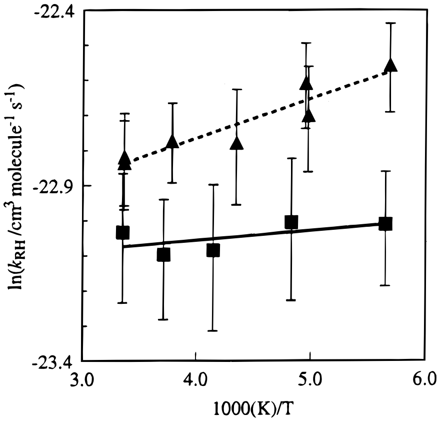

Figure 4. Arrhenius plot: ■, C_2H + isobutane ($k_{isobutane} = (8.7 \pm 0.8) \times 10^{-11} \exp(28 \pm 21/T)$ cm^3 molecules^{-1} s^{-1}); ▲, C_2H + *n*-butane ($k_{n-butane} = (8.3 \pm 0.6) \times 10^{-11} \exp(112 \pm 18/T)$ cm^3 molecules^{-1} s^{-1}).

7.9×10^{-11}, $k_{isobutane} = 9.6 \times 10^{-11}$, $k_{n-butane} = 1.2 \times 10^{-10}$, $k_{neopentane} = 1.1 \times 10^{-10}$ cm^3 molecules^{-1} s^{-1}. (Uncertainty associated with Arrhenius expressions is the computed standard error of the fit to the two parameters.) Although the lowest experimental temperature is approximately 150 K, rate constants could only be determined for isobutane, *n*-butane, and neopentane above 170 K. Attempts to measure the reaction rates at lower temperature were prevented because of the apparent saturation of the RH concentration, most likely due to wall condensation. The rate coefficients are independent of pressure over the range 1.3−12 kPa total pressure ($[C_2H_2] = (2-6) \times 10^{14}$ cm^{-3}, $[RH] = (1.0-1.5) \times 10^{15}$ cm^{-3}, balance helium).

Discussion

There are two previously reported values for the reaction of C_2H + propane.[16,17] Figure 3 demonstrates the large uncertainty associated with the estimated value of Tsang and the discrepancies with the current work. Tsang[17] indicated that there was no data available for this reaction. However, Okabe[16] published two papers that include this reaction. In these previous experiments, acetylene was photolyzed at 184.9 nm and the production of diacetylene (C_4H_2) was measured by absorption at ~165 nm with and without the presence of propane. By combining eq 6 with the equation for diacetylene formation

$$C_2H + C_2H_2 \rightarrow C_4H_2 + H \tag{18}$$

the following relation was derived:

$$\frac{\phi^0(C_4H_2)}{\phi(C_4H_2)} = 1 + \frac{k_{propane}[C_3H_8]}{k_{acetylene}[C_2H_2]} \tag{19}$$

where $\phi(C_4H_2)$ and $\phi^0(C_4H_2)$ symbolize the quantum yield of the diacetylene with and without propane, respectively.[16] The ratio $k_{propane}/k_{acetylene}$ was then determined to be (0.469 ± 0.041) and $k_{propane}$ calculated from a previously determined value of $k_{acetylene}$. Comparison of the originally published value of $k_{propane}$ with that determined here shows a discrepancy of a factor of ~5. However, substituting the most recent value of $k_{acetylene}$[11,15] into eq 19 produces a rate constant that is in good agreement with our experimental results.

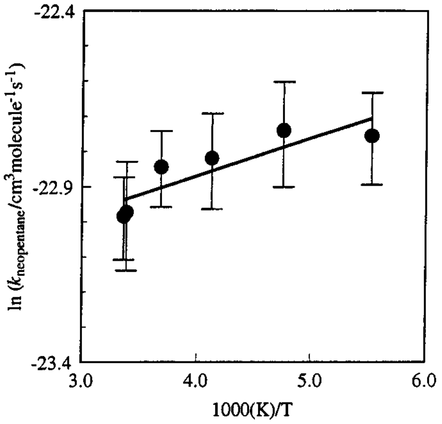

Figure 5. Arrhenius plot for C_2H + neopentane: $k_{neopentane} = (7.6 \pm 0.9) \times 10^{-11} \exp(107 \pm 30/T)$ cm^3 molecules^{-1} s^{-1}

TABLE 2: Comparison of Literature Values for Rate Constants of C_2H + RH

$C_2H + C_3H_8$	$k_{propane}$ (cm^3 molecules^{-1} s^{-1})	temp (K)
this work[a]	7.9×10^{-11}	298
Okabe[b]	$(1.4 \pm .1) \times 10^{-11}$	298
Okabe[c]	7.4×10^{-11}	
Tsang[17]	5.2×10^{-12} (estimate)	300−2500
C_2H + *i*-C_4H_{10}	$k_{isobutane}$ (cm^3 molecules^{-1} s^{-1})	temp (K)
this work[a]	9.6×10^{-11}	298
Tarr[20]	only ratio given	
Tsang[18]	9.1×10^{-12} (estimate)	300−2500
C_2H + *n*-C_4H_{10}	$k_{n-butane}$ (cm^3 molecules^{-1} s^{-1})	temp (K)
this work[a]	1.2×10^{-10}	298
Tarr[20]	only ratio given	
C_2H + *neo*-C_5H_{12}	$k_{neopentane}$ (cm^3 molecules^{-1} s^{-1})	temp (K)
this work[a]	1.1×10^{-10}	298
Cullis[21]	only ratio given	

[a] Calculated from Arrhenius expression. [b] From ref 16. Published value with $C_2H + C_2H_2$ rate coefficient of 3×10^{-11} cm^3 molecules^{-1} s^{-1}. [c] From ref 16. Recalculated using $C_2H + C_2H_2$ rate coefficient of 1.4×10^{-10} cm^3 molecules^{-1} s^{-1} from ref 15.

Tsang also made an estimate for the rate constant of C_2H + isobutane.[18] The value was estimated to be 1.5 times the rate constant for C_2H + ethane. However, the value determined here is an order of magnitude faster than this estimate. The estimated value is included in Figure 3 for reference rather than in Figure 4 so that the Figure 4 scale can have better resolution. Using the most recent rate constant for C_2H + ethane (3.5×10^{-11} cm^3 molecules^{-1} s^{-1}),[19] Tsang's method of estimation gives a predicted rate constant for isobutane that is low by only a factor of 2. Further comparison with previous work on C_2H with isobutane, *n*-butane, and neopentane is difficult, since only a ratio of the rates compared with a standard ($C_2H + BrC_2H$) was given.[20,21] A search of a recent chemical kinetics data base and the literature failed to provide the needed rate constant for comparison. Comparisons of available rates are summarized in Table 2.

The measured rate coefficients for isobutane, *n*-butane, and neopentane are the first C_2H + alkane reactions to demonstrate a negative temperature dependence. Sims et al. have reported a negative temperature dependence for the reaction $CN + C_2H_6 \rightarrow$ products. However, the rate constant only begins to show a negative temperature dependence at temperatures below ~75 K.[22] A similar negative temperature dependence has also been observed in the recent work with C_2H + acetylene[11] and C_2H + ethylene.[19] These results are attributed to an addition−elimination mechanism. The corresponding processes in C_2H + RH for addition/elimination are exothermic by ~100 kJ/mol (eqs 9−12), but the possibility of such a mechanism involving attack of a J-bond or saturated carbon seems highly unlikely. The relatively low C_2H and RH concentrations, coupled with temperatures above 170 K, would also preclude the formation of stabilized van der Waals complexes. Sims et al. have proposed that formation of a *transient* van der Waals complex

TABLE 3: Comparison of Rate Constants of C_2H + RH with Those Used in Planetary Models (Rate Constant k_{RH} in cm^3 molecules^{-1} s^{-1})

reaction	this work[a] (T = 140 K)	Yung et al.	Toublanc et al.	Gladstone et al.
$C_2H + C_3H_8 \rightarrow C_2H_2 + C_3H_7$	8.0×10^{-11}	1.4×10^{-11} [b]	6.0×10^{-12} [c]	1.4×10^{-11} [b]
$C_2H + n\text{-}C_4H_{10} \rightarrow C_2H_2 + C_4H_9$	1.8×10^{-10}			1.4×10^{-11} [b]
$C_2H + i\text{-}C_4H_{10} \rightarrow C_2H_2 + C_4H_9$	1.1×10^{-10}			1.4×10^{-11} [b]

reaction	previous work[d] (T = 140 K)	Yung et al.	Toublanc et al.	Gladstone et al.
$C_2H + CH_4 \rightarrow C_2H_2 + CH_3$	3.6×10^{-13}	4.7×10^{-13}	5.0×10^{-13}	1.5×10^{-12}
$C_2H + C_2H_6 \rightarrow C_2H_2 + C_2H_5$	3.6×10^{-11}	6.5×10^{-12}	3.6×10^{-11}	2.1×10^{-11}

[a] Calculated from Arrhenius expressions. [b] From Okabe, ref 16. [c] From Tsang, ref 17. [d] Calculated from Arrhenius expressions, refs 11,19.

can enable the reactants to find a favorable orientation for reaction to occur when the energy of the colliding species is comparable to or lower than the depth of the van der Waals well.[22] As a first approximation, the depth of the "well" on the C_2H−RH Lennard-Jones potential can be estimated using the combining rule.[23] (C_2H is assumed to have the same Lennard-Jones parameters as C_2H_2.[24]) The well depths, ϵ/k_b (where k_b is the Boltzmann constant), for C_2H/propane, isobutane, and n-butane are estimated to be 212−217, 240, and 234−275 K, respectively. (The ranges for the values of ϵ/k_b arise from the difference in Lennard-Jones parameters determined from second virial coefficients and viscosity data.) The values for isobutane and n-butane are quite large when compared to the ϵ/k_b value of 160 K calculated for CN/ethane. Based on this approximation and the hypothesis but forth by Sims et al., the observed negative temperature dependence can possibly be explained. However, further investigation of the role that weak, long-range, attractive forces have on chemical reactions at low temperatures is needed.

Since one of the main goals of these measurements is to provide low-temperature rate coefficients for use in planetary atmospheric models, it is valuable to make a comparison with the rate coefficients that have been used previously. The measured rate coefficients for the current set of experiments are faster by a factor of 5−10 than those used in the photochemical models. Experimental results for C_2H + methane[11] and ethane[19] show up to an order of magnitude difference from values previously used in the models. These comparisons are summarized in Table 3. (The temperature of 140 K is chosen for the comparison based on the altitude of the observational data and the calculated thermal profile on Titan.[7]) As mentioned above, the rate coefficient for propane has no temperature dependence, while those for isobutane, n-butane, and neopentane show a slight negative temperature dependence. Therefore, room-temperature (or slightly higher-temperature) rate constants could be used in the absence of low-temperature data for these reactions. Yung et al.[6] and Gladstone et al.[3] used the published value of Okabe[14] (see Tables 2 and 3) for the reaction of C_2H + propane. Yung et al. were internally consistent, using the same value for the rate constant for C_2H + acetylene as that used by Okabe (3×10^{-11} cm^3 molecules^{-1} s^{-1}). However, Gladstone et al. continued to use the value given by Okabe for C_2H + propane while employing a new value for the C_2H + acetylene reaction (1.5×10^{-10} cm^3 molecules^{-1} s^{-1}). As discussed above, the adjustment with the recent measurements of C_2H + acetylene[11,15] places the C_2H + propane rate constant of Okabe very close to the value reported here. Toublanc et al. used the estimated value of Tsang,[17] which, as discussed above, is over an order of magnitude lower than the experimentally determined value measured here.

Gladstone et al. extended their model of the hydrocarbon photochemistry of Jupiter to include C_3 and C_4 species. They estimated the reaction of $C_2H + C_4H_{10}$ to be equal to that used for propane. The current measurements show that both isomers of butane have a slightly faster reaction rate than propane at room temperature. From the corresponding Arrhenius expressions for n-butane, which shows the largest negative temperature dependence, the rate would increase by a factor of 2 from 298 to 140 K, the colder temperature being more closely related to that on Titan. Efforts are currently under way to extend our low-temperature measurements even further.

The rate coefficients measured here are higher than those currently used in all of the photochemical models. Faster rates would predict higher C_3 and C_4 radical concentrations and consequently increase concentrations of larger molecular weight hydrocarbons. The upcoming Cassini/Huygens mission to Saturn and Titan will answer many of the questions regarding the presence (or absence) of larger hydrocarbons in Titan's atmosphere.

References and Notes

(1) Kern, R. D.; Xie, K. *Prog. Energy Combust. Sci.* **1991**, *17*, 191.

(2) Moortgat, G. K.; Barnes, A. J.; Le Bras, G.; Sodeau, J. R., Eds. *Low-Temperature Chemistry of the Atmosphere*; Springer-Verlag: New York, 1994.

(3) Gladstone, G. R.; Allen, M.; Yung, Y. L. *Icarus* **1996**, *119*, 1.

(4) Raulin, F.; Bruston, P.; Coll, P.; Coscia, D.; Gazeau, M.-C.; Guez, L.; de Vanssay Lisa, E. *J. Biol. Phys.* **1994**, *20*, 39.

(5) Toublanc, D.; Parisot, J. P.; Brillet, J.; Gautier, D.; Raulin, F.; McKay, C. P. *Icarus* **1995**, *113*, 2.

(6) Yung, Y. L.; Allen, M.; Pinto, J. P. *Astrophys. J., Suppl. Ser.* **1984**, *55*, 465. Yung, Y. L. *Icarus* **1987**, *72*, 468.

(7) Coustenis, A.; Bézard, B.; Gautier, D.; Marten, A.; Samuelson, R. *Icarus* **1991**, *89*, 152.

(8) Cabane, M.; Chassefière, E. *Planet. Space Sci.* **1995**, *43*, 47.

(9) Weast. R. C., Ed. *CRC Handbook of Chemistry and Physics*; CRC: Boca Raton, 1990. Lowry, T. H.; Richardson, K. S. *Mechanisms and Theory in Organic Chemistry*; Harper and Row: New York, 1987.

(10) Pedersen, J. O. P.; Opansky, B. J.; Leone, S. R. *J. Phys. Chem.* **1993**, *97*, 6822.

(11) Opansky, B. J.; Leone, S. R. *J. Phys. Chem.* **1996**, *100*, 4888.

(12) Hall, J. L.; Lee, S. A. *Appl. Phys. Lett.* **1976**, *29*, 367.

(13) Satyapal, S.; Bersohn, R. *J. Phys. Chem.* **1991**, *95*, 8004.

(14) Shin, K. S.; Micahael, J. V. *J. Phys. Chem.* **1991**, *95*, 5864.

(15) Opansky, B. J. Low Temperature Rate Coefficients of the Ethynyl Radical, C_2H. Ph.D. Thesis, University of Colorado, Boulder, CO, 1996.

(16) Okabe, H. *J. Chem. Phys.* **1983**, *78*, 1312. Okabe, H. *Can. J. Chem.* **1983**, *61*, 850.

(17) Tsang, W. *J. Phys. Chem. Ref. Data* **1988**, *17*, 887.

(18) Tsang, W. *J. Phys. Chem. Ref. Data* **1990**, *19*, 1.

(19) Opansky, B. J.; Leone, S. R. *J. Chem. Phys.*, submitted.

(20) Tarr, A. M.; Strausz, O. P.; Gunning, H. E. *Trans. Faraday Soc.* **1965**, *61*, 1946.

(21) Cullis, C. F.; Hucknall, D. J.; Shepherd, J. V. *Proc. R. Soc. London, Ser. A* **1973**, *335*, 525.

(22) Sims, I. R.; Queffelec, J. L.; Travers, D.; Rowe, B. R.; Herbert, L. B.; Karthäuser, J.; Smith, I. W. M. *Chem. Phys. Lett.* **1993**, *211*, 461.

(23) Smith I. W. M. *Kinetics and Dynamics of Elementary Gas Reactions*; Butterworth: London, 1980; p 47.

(24) Hirshfelder, J. O.; Curtiss, C. F.; Bird, R. B. *The Molecular Theory of Gases and Liquids*; Wiley: New York, 1954; p 1112.